electronics

MDPI

Article

UWB-Based Accelerometer Sensor Nodes for Low-Power Applications in Offshore Platforms

Markos Losada [1], Aitor Olaizola [1], Andoni Irizar [1,2], Iker Fernández [1], Adrián Carrasco [1], Joep Van der Zanden [3] and Ainhoa Cortés [1,2,*]

[1] CEIT-Basque Research and Technology Alliance (BRTA), Manuel Lardizabal 15, 20018 Donostia-San Sebastian, Spain; mlosada@ceit.es (M.L.); aolaizolapa@ceit.es (A.O.); airizar@ceit.es (A.I.); ifernandezand@ceit.es (I.F.); acarrascoro@ceit.es (A.C.)
[2] Department of Electronics and Communications, Universidad de Navarra, Tecnun, Manuel Lardizabal 13, 20018 Donostia-San Sebastian, Spain
[3] Maritime Research Institute Netherlands (MARIN), 6708 PM Wageningen, The Netherlands
* Correspondence: acortes@ceit.es; Tel.: +34-943212800

Abstract: Due to the growth of renewable energies, which requires cost reduction and efficiency in terms of structural health assessment, failure prevention, effective maintenance scheduling, and equipment lifespan optimization, in this paper, we propose an Ultra Wideband (UWB)-based accelerometer Sensor Node for low-power applications in offshore platforms. The proposed Sensor Node integrates a high-resolution accelerometer together with an Impulse Radio Ultra-Wideband (IR-UWB) transceiver. This approach enables effective remote monitoring of structural vibrations. This provides an easy-to-install, scalable, and flexible wireless solution without sacrificing robustness and low power consumption in marine environments. Additionally, due to the diverse and highly demanding applications of condition monitoring systems, we propose two modes of operation for the Sensor Node. It can be remotely configured to either transmit raw data for further analysis or process data at the edge. A hardware (HW) description of the proposed Sensor Node is provided. Moreover, we describe the power management strategies implemented in our system at the firmware (FW) level. We show detailed power consumption measurements, including power profiles and the battery-powered autonomy of the proposed Sensor Node. We compare data from a wired acquisition system and the proposed wireless Sensor Node in a laboratory environment.The wired sensor integrated into this acquisition system, fully characterized and tested, is our golden reference. Thus, we validate our proposal. Furthermore, this research work is within the scope of the SUREWAVE Project and is conducted in collaboration with the MARIN Institute, where wave basin tests are carried out to evaluate the behavior of a Floating Photovoltaic (FPV) system. These tests have provided a valuable opportunity to assess the effectiveness of the proposed Sensor Node for offshore platforms and to compare its performance with a wired system.

Keywords: hostile environments; low power consumption; wireless sensors; ultra-wide band; marine platforms; accelerometers; vibrations; loads; edge computing

Citation: Losada, M.; Olaizola, A.; Irizar, A.; Fernández, I.; Carrasco, A.; Zanden, J.V.d.; Cortés, A. UWB-Based Accelerometer Sensor Nodes for Low-Power Applications in Offshore Platforms. *Electronics* **2024**, *13*, 4485. https://doi.org/10.3390/electronics13224485

Academic Editor: Andrea Bonci

Received: 4 October 2024
Revised: 12 November 2024
Accepted: 13 November 2024
Published: 15 November 2024

1. Introduction

In the renewable energy sector, offshore wind is rapidly acquiring an important role because it can deliver power consistently and predictably at a highly competitive cost, as well as having greater space availability and avoiding the environmental impact of inland wind generators [1,2].

To achieve the European Commission's 2030 target of 40% of renewable energy in the energy mix, the levelized cost of energy (LCoE) in offshore wind farms (OWF) must be reduced [3].

The operational maintenance cost is the main recurring cost in wind power and must be reduced without compromising its long-term operation. To achieve this goal, continuous

remote monitoring of critical components of the system will have a key role. By placing sensors (vibrations, loads, corrosion, etc.) in key locations in the structure and remotely accessing the data, it would be possible to minimize the number of on-site inspections, for example. In addition, by continuously monitoring the condition of the wind turbines, operators can schedule maintenance more effectively, minimizing downtime and extending the useful life of the equipment [4,5].

Sensors used for continuous monitoring must meet several requirements. They must run with very limited power (and ideally, be battery powered), have easy installation and maintenance (battery will need to be changed someday), use wireless communications to facilitate the deployment, and be very robust against the harsh environment (salinity, waves, temperatures, UV exposure, etc). This can be achieved when monitoring variables that change very slowly (temperature, salinity, corrosion, coating degradation, etc.) and, therefore, need just a few measurements per day.

Monitoring vibrations in offshore wind generators using wireless accelerometers is an effective method for structural health assessment, which can lead to reduced maintenance costs. These accelerometers are capable of detecting the full range of vibrational frequencies produced during wind turbine operation, allowing for the identification of faults and structural flaws. Hence, the condition of wind turbines can be assessed remotely and accurately in real-time, minimizing the need for on-site engineers. This not only improves safety by reducing human intervention, but also improves data collection, leading to more efficient maintenance strategies that consider the dynamic and environmental loads affecting the turbines [6–8].

However, vibration monitoring presents additional challenges because it requires a continuous sampling of the accelerations taking place in the structure, which obliges the sensor to be active during far longer periods of time than other sensors.

Wireless accelerometers have numerous advantages over traditional wired accelerometers. Firstly, the absence of cables simplifies installation and enhances flexibility. In spite of the higher initial cost compared to wired counterparts, wireless accelerometers can yield cost savings in the long term due to reduced labor and material expenses associated with cables. In addition, the durability and longevity of wireless accelerometers are improved as they eliminate the risk of cable wear and damage, requiring less maintenance. Furthermore, wireless accelerometers are easier to scale up or expand to monitor multiple points simultaneously, making them ideal for large-scale monitoring applications. However, the data gathered by vibration sensors are large (even huge) and must be sent to other devices for further analysis using wireless communications that employ large amounts of energy, which makes them very dependent on stored energy (batteries) for operation or harvesting solutions. Frequent battery replacement will nullify any cost savings accomplished by using wireless sensors. Therefore, reducing power consumption is a top priority in wireless accelerometers [9].

In essence, in addition to the requirements that this type of sensor must meet, such as being compact, robust, wireless, and cost-effective, there are other issues raised in the literature that need to be addressed, particularly those related to power strategies and data management, to achieve low-power solutions and thereby extend the battery life of the sensors. Furthermore, it is essential to evaluate the suitability of this type of system in a marine environment in terms of robustness. This paper presents an instance of such wireless accelerometer technology, designed for remote sensing and data transmission, resistance to the harsh, humid, and corrosive marine environment, and optimized for low energy consumption. It is also capable of performing a degree of edge processing.

2. Related Work

The maintenance of offshore wind energy platforms is challenging due to harsh environmental conditions and their remote locations. Conventional maintenance strategies can lead to unsustainable costs, thereby reducing the return on investment (RoI). To contribute to the growth of offshore wind energy as a highly profitable renewable energy

option, an intelligent monitoring system, like the ones described in [4–8,10,11], should be implemented. Some of these types of monitoring system can reduce the need for on-site inspections and enhance data collection, leading to more effective maintenance strategies. Nevertheless, many of these systems are not optimized for power consumption and struggle to effectively manage large amounts of data. Furthermore, there are very few instances where deployment in real-world environments has been successfully carried out. Below, technologies, methods, and mechanisms found in the literature that help achieve a robust, remote, low-power, low-cost and intelligent monitoring system will be reviewed.

Wireless Sensor Network (WSN) architecture is the most practical choice for an offshore platform monitoring system. In contrast to wired options, it allows for cost-effective installations in remote and harsh environments for temporary, mobile, or permanent applications [12–14]. Nevertheless, selecting the most suitable technology for a WSN can be challenging due to varying communication system requirements. Refs. [15] evaluate the specific conditions and requirements for WSNs in challenging offshore environments. Ref. [16] discusses the critical points of WSNs applied in structural monitoring systems, while in [17], a comparison between different technologies for WSNs is shown. For offshore monitoring systems, Impulse Radio Ultra-Wideband (IR-UWB) is considered the most viable technology in the case of WSNs because of its high time-domain resolution, low-power, and cost-effective characteristics [15,17,18].

In addition to communication technology, the selection of appropriate sensors is crucial and should align with the required specifications, which are derived from the specific use case. Matching the sensors to the exact needs of the application ensures optimal performance and data accuracy in the overall system. This becomes even more critical when implementing sensors for measuring dynamic movements, such as accelerometers. Therefore, an appropriate methodology and a relevant environment are necessary to validate the performance of the accelerometer. Ref. [19] introduces a wireless accelerometer for structural health monitoring, outlining the challenges of hardware and software integration and discussing associated resolutions. The experimental performance of the wireless accelerometer is validated by comparing it with high-sensitivity wired accelerometers. In [20], an enhanced low-cost triaxial accelerometer is presented. With increased bandwidth, standalone capability, reduced noise density, and internet-based synchronization, it aims to make Structural Health Monitoring (SHM) more affordable and applicable to a wider range of structures. The tests conducted to validate the system's accuracy across various frequencies and amplitudes are examined. Ref. [21] focuses on the synchronization of a wireless accelerometers network to ensure precise condition assessment of structures and minimize false-positive damage indications. Ref. [22] introduces a novel method utilizing wireless high-resolution acceleration sensors to analyze the vibration response of wind turbine towers. It demonstrates how the resolution of acceleration and the placement of Sensor Nodes affect the accuracy of eigenfrequency determination. A comparison is provided between data from wireless Sensor Nodes and wire counterparts to validate the wireless sensing approach. Additionally, the paper explores data compression techniques for minimizing wireless transmission requirements. It must be noted that these works have not emphasized the development of a compact, low-power, and cost-effective sensor design.

Deploying wireless sensors entails effectively handling the large volume of data they produce, especially when operating in very restricted energy availability conditions. Therefore, implementing power-saving strategies and employing intelligent data management are key considerations. Some works in the literature [23,24] address the strategy for powering WSN systems as a major challenge. Ref. [23] shows a set of test results that assisted in optimizing the amount of data collected per measurement. Minimizing the information transmitted by the nodes can help reduce the power consumption associated with these communications. In this context, Ref. [25] introduces a fault detection system with adaptive thresholds that efficiently minimizes the size of data packets sent by Sensor Nodes. This approach not only saves energy but also enhances the node lifetime by optimizing data transmission and reducing unnecessary communications.

Edge computing represents a new approach to efficiently managing data from sensor networks. The change in perspective is intended to reduce network congestion and improve performance by locating computing and storage resources in close proximity to the data source [26]. Before deploying edge computing infrastructure, it is essential to thoroughly explore and investigate the energy and power efficiency of the underlying hardware. Edge computing platforms must be designed focusing on energy efficiency to fulfil application requirements while minimizing energy consumption and costs. A trade-off needs to be made between the duration of the event to be communicated and the intensity of usage in order to optimize performance. Ref. [27] presents a survey that examines various factors to consider in edge and fog devices to reduce energy consumption, thereby extending the lifespan of both the devices and the network. Ref. [24] introduces a flexible fog computing design for low-power consumption and low-latency applications. In this approach, the WSN is equipped to intelligently select the most suitable radio technology for various types of data communication. The proposed multi-technology network considers factors such as the volume of data to be transmitted, the necessary data rate, and the coverage range to determine the optimal communication method. Recently, in [28], an overview of edge devices, edge servers, and cloud data centers was provided. The article reviews the latest research on energy-efficient edge computing and explores related research challenges and future directions, covering areas such as operating systems, middleware, applications, and computation offloading. In [29], a comprehensive assessment of the performance of various single-board computer platforms frequently used in IoT systems is conducted. The objective was to conduct a comprehensive performance evaluation aimed at determining the viability of deploying virtualized instances efficiently on single-board computers. However, most of these works do not provide the power consumption measurements of their approach. But above all, almost all of them do not validate their proposal in a relevant maritime environment.

In summary, we have found different offshore platform monitoring systems relying on different communication methods. It is shown that the nature of the WSN makes them the most suitable option to be implemented. The scalability of WSN allows for easier expansion to monitor multiple points simultaneously, and also simplifies installation and maintenance. One wireless communication technology that excels in harsh and variable environments is Impulse Radio Ultra-Wideband (IR-UWB). This technology has demonstrated good flexibility and robustness in communication links, making it an ideal choice for such deployments. In the literature review, WSNs based on accelerometers were identified, and an in-depth analysis was conducted to evaluate their performance. The aim was to determine how well these accelerometers functioned in capturing and transmitting data related to dynamic movements, such as vibrations or structural changes, in the monitored environment. Such an analysis is crucial for understanding the capabilities and limitations of accelerometer-based WSN systems in practical applications. However, these designs are either not optimized or are not yet suitable for implementation in a real-world environment. On the other hand, implementing power-saving strategies and utilizing intelligent data management techniques are crucial factors to consider when designing and deploying systems that involve WSNs. These strategies help optimize energy efficiency, prolong battery life, and enhance overall system performance. Under the concept of edge computing, very specific embedded systems are utilized to handle data processing tasks, reducing the dependence on cloud processing or communication. This strategy reduces latency and power usage by distributing the frequency and volume of transmissions. The literature shows that edge computing demands low-power devices that are capable of self-reprogramming and self-reconfiguration, enabling them to adjust energy consumption according to various hardware and software platforms. However, some designs mentioned in the literature are either not optimized for a maritime environment or do not demonstrate actual power consumption results.

The literature review shows us that there are works dealing with intelligent monitoring systems for offshore platforms; however, most of them are not designed to face such a

challenging and remote environment. Some others are proof-of-concept or even theoretical works. Therefore, in this work, we aim to provide a solution that can address issues such as remote monitoring, robustness, power consumption, and which represents a low-cost approach to support an intelligent monitoring system. Hence, we introduce a UWB-based accelerometer Sensor Node designed for monitoring offshore structures, featuring low power consumption, edge computing capabilities, reconfigurability, robustness, and cost-effectiveness. Furthermore, the performance of the proposed node is validated in both laboratory and maritime environments.

3. Case Study: Monitoring Floating Breakwater Designed to Protect Offshore FPV

The target case study for the work presented in this paper is to monitor the loads and vibrations of the breakwater designed in the scope of the SUREWAVE Project.

The primary aim of SUREWAVE is to develop and test an innovative Floating Photo-Voltaic (FPV) system. This system features an external floating breakwater structure made from new circular materials, designed to protect the FPV structure from severe wave impacts, thereby enhancing operational availability and energy production. This concept is capable of functioning in all European sea basins, including extremely harsh open-sea environments with high winds (speeds over 25 m/s), strong currents (over 1.2 m/s), and large waves (heights over 14 m). This advancement could facilitate the widespread deployment of offshore FPV systems both in Europe and globally.

Therefore, the structural integrity of the breakwater becomes extremely crucial and the idea of measuring the loads/vibrations of this reinforced concrete structure in real-time is very relevant. To achieve this continuous monitoring, low-cost and robust Sensor Nodes must be deployed on the structure. To facilitate the deployment of these Sensor Nodes on the offshore FPV platforms operating in open-sea conditions, the integration of Sensor Nodes with wireless capabilities is key. Thus, the installation costs are reduced considerably in terms of time and effort. On the other hand, the wireless link must be robust enough to operate in such harsh environments.

In [30], the wave basin tests of a multi-body floating PV system sheltered by a floating breakwater are presented. The main aim of these tests conducted by MARIN was to extend insights into the hydrodynamic behavior (motion response and hinge loads) of multi-body FPV systems, especially in harsh environments with mild and harsh waves. Apart from this, CEIT used the wave basin tests to evaluate the performance of the UWB-based accelerometer Sensor Node proposed in this paper. This was a relevant scenario to test the robustness of the proposed approach for offshore platforms and the performance was compared to the acquisition wired system used by MARIN for the hydrodynamic analysis. The results obtained during these tests are presented in Section 6.3.

4. SUREWAVE System Architecture

The proposed system architecture is shown in Figure 1.

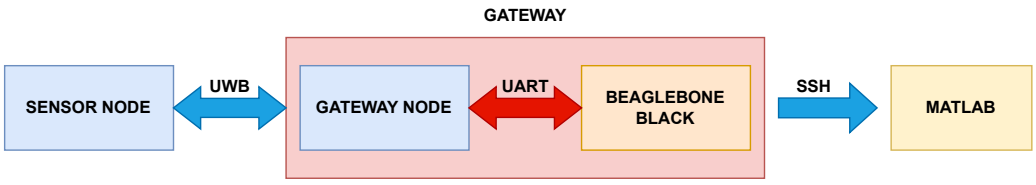

Figure 1. SUREWAVE system architecture.

The SUREWAVE system is mainly formed by three modules: the Sensor Node, the Gateway (formed by a Gateway Node and a BeagleBone Black) and a post-processing system with MatLab. Particularly, this paper will focus on the design of the Sensor Node and its communication with the Gateway. The architecture and integration of this system will be explained in the following sections.

The system was designed with the goal of leveraging the versatility of the accelerometer, allowing for measurements at different sampling frequencies. This capability to choose the sampling frequency is further enhanced by the configurable UWB link between the Sensor Node and the Gateway. This link can be adjusted by modifying the preamble length and data rate to suit the use case. The UWB configuration will have a direct impact on the maximum sampling frequency capacity, as higher frequencies will necessitate faster data transmission.

The system offers two types of data processing: Packet and Edge. On the one hand, in the Packet mode, data are sent from the Sensor Node to the Gateway for later processing and visualization in an external program such as Matlab r2023b. On the other hand, in the Edge mode, the data are processed at the Sensor Node. Both types of data processing will influence the final energy consumption as will be discussed later.

The topology and message exchange of the Sensor Node are shown in Figure 2:

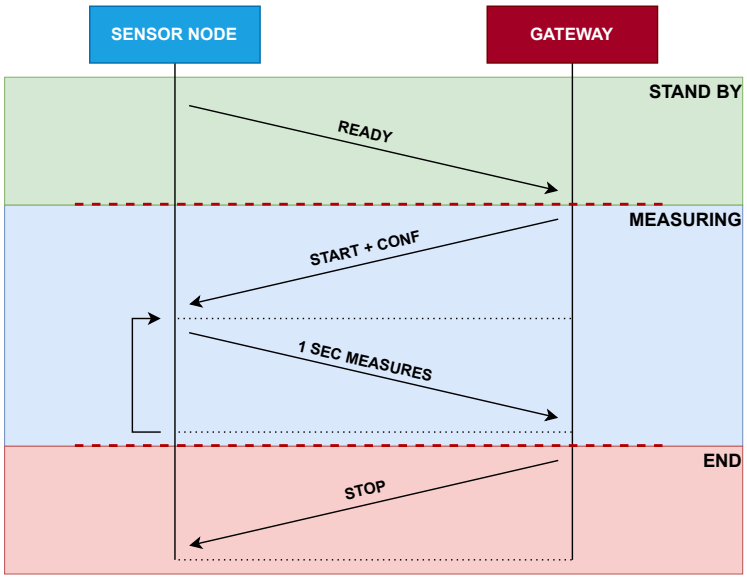

Figure 2. SUREWAVE comunication topology.

- STANDBY: In this mode, the objective is to keep the Sensor Node in a sleep state for as long as possible when it is not in use. While asleep, the Sensor Node will consume extremely little power, waking up periodically to send a "READY" message. If the Gateway responds, the Sensor Node will configure various parameters according to the system requirements and go to the next mode, 'MEASURING'. If no response is received from the Gateway, the Sensor Node will return to the sleep state in 'STANDBY' mode.
- MEASURING: In this mode, it is essential for the Sensor Node to continuously measure and locally store the accelerometer data. After one second, the UWB module is activated and transmits the measurements in parallel while the accelerometer continues to take readings. Once the data are transmitted, the DW1000 (UWB integrated circuit) goes back to the sleep state until the next transmission event (another second of data storage). This process will continue until the Sensor Node receives a "STOP" command from the Gateway. In the case of Edge mode, the duration of the measurement event will be determined by the window time.

4.1. The Sensor Node

- **Hardware**

  Figure 3 shows the architecture of the Sensor Node.

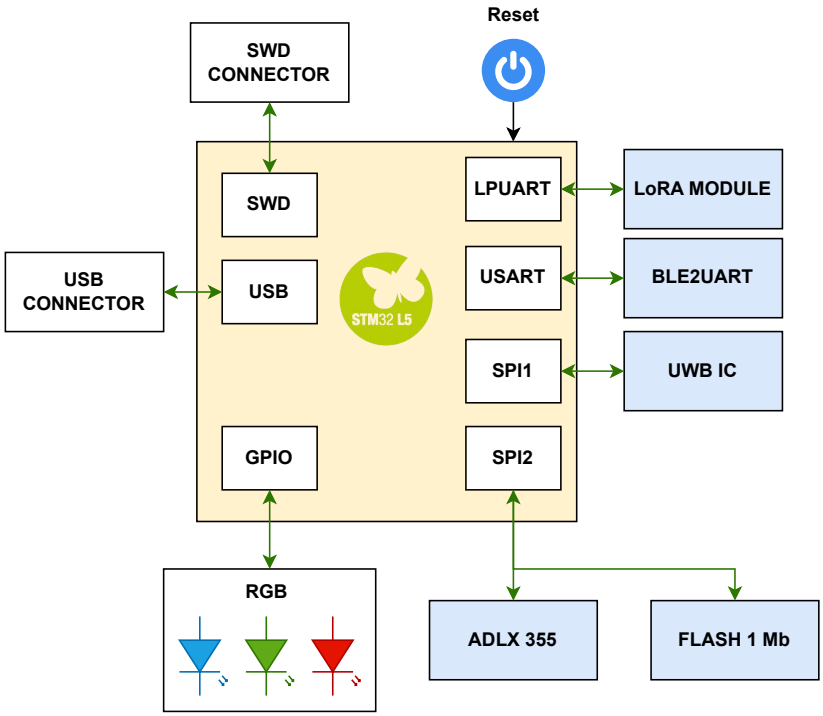

Figure 3. Sensor Node architecture.

A custom board was designed for this architecture based on the STM32L552 microcontroller serving as the processing and control core. One of its best features is its low power consumption in STANDBY mode.

Based on the system used in [17], the board is equipped with IR-UWB technology through a DW1000 integrated circuit from Decawave [31], an IEEE 802.15.4-2011 UWB compliant, low-power, low-cost wireless transceiver.

In this setup, the Sensor Node uses UWB technology to send accelerometer measurements to the Gateway. The IEEE 802.15.4 UWB PHY has 16 defined channels, with the DW1000 IC supporting channels 1, 2, 3, 4, 5, and 7. Additionally, the integrated circuit can handle data rates of 110 kbps, 850 kbps, and 6800 kbps. These parameters will be configured by the user in the application. It will be necessary to balance the sampling rate of the accelerometer and the data rate of the UWB transceiver to prevent losing samples in the process.

The ADXL355 [32] is a 3-axis MEMS accelerometer known for its low noise density, low 0g offset drift, and low power consumption, featuring selectable measurement ranges. It supports up to ±8 g range, providing industry-leading noise performance and long-term reliability. This enables precise applications with very low power usage.

Figure 4 shows a photo of the designed board.

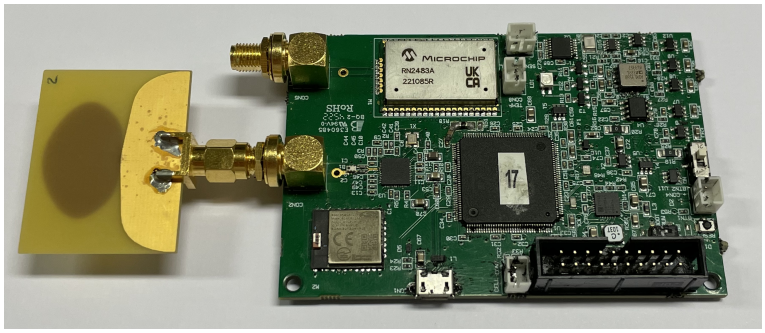

Figure 4. Sensor Node board.

- **Firmware**

One important challenge of this Sensor Node is to reduce as much as possible the power consumption of the complete device, since it will be powered by an external battery. For this purpose, an autonomous timer was implemented. This timer will take care of the events of sleeping and waking up the Sensor Node. Then, two power management modes were implemented: STANDBY and MEASURING. The behavior of these power management modes is illustrated in the Figure 5, which shows the flowchart of the firmware implemented in the microcontroller.

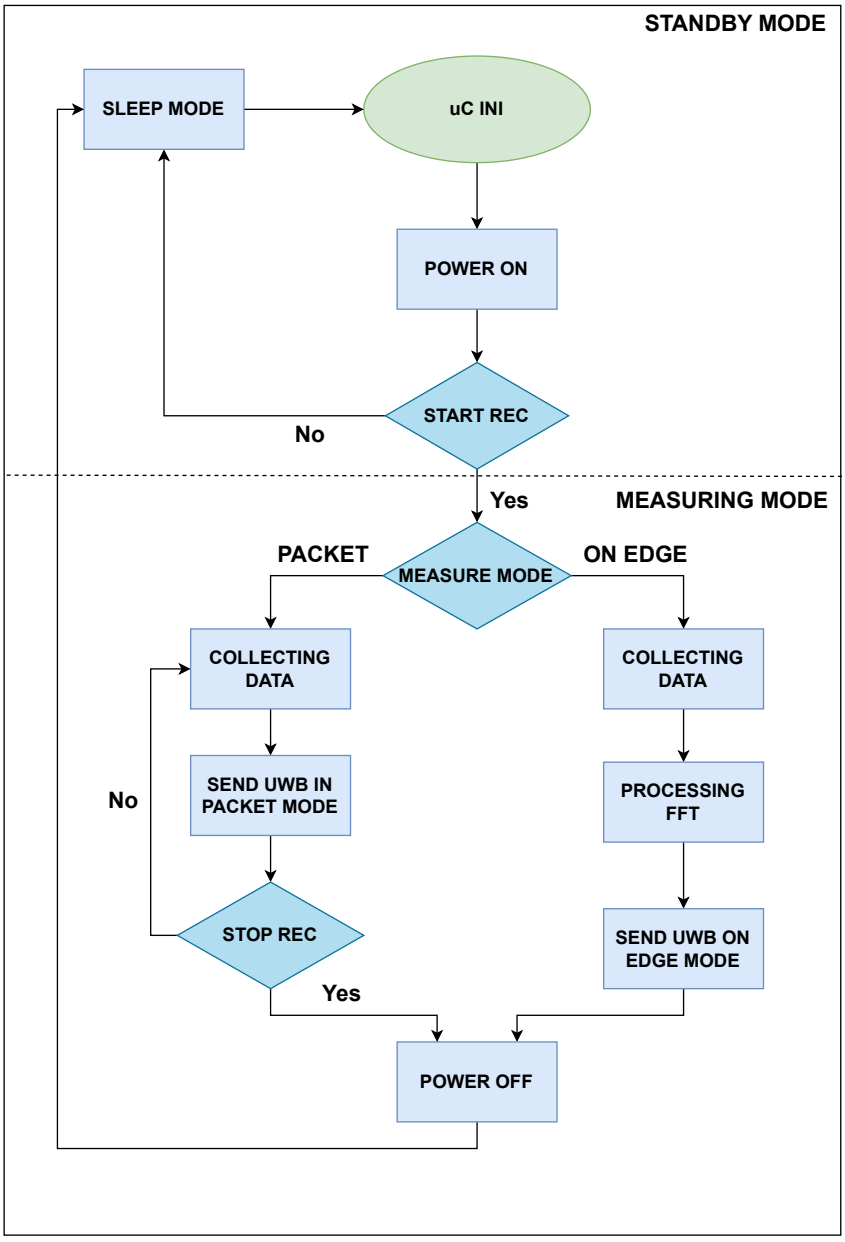

Figure 5. Sensor Node flow chart.

In the case of the STANDBY mode, the Sensor Node performs the following tasks after being woken-up: initializing the microcontroller, configuring the UWB interface, sending a 'READY' message via UWB to tell the Gateway that it is ready, disabling the power supplies and going back to STANDBY. The Sensor Node performs this wake-up event every *T-off* seconds until it receives a response from the Gateway to the 'READY' message, in which case it goes into MEASURING mode.

Once inside the MEASURING mode, the program offers two modes for data processing. On the one hand, the Packet mode, in which raw data are sent to the Gateway for further processing, and on the other hand, the Processing On Edge mode, in which the data are processed on the Sensor Node itself. The operation of both modes is described below:

- **Packet mode:** In this mode the Sensor Node activates the accelerometer so that it is constantly making measurements at the desired frequency. After one second of measurements, the UWB transceiver is woken up and the measurements are sent to the Gateway in packets of 100 bytes. These packets contain information from all three axes of the accelerometer along with a time stamp and the sample index. One measurement with this information takes 20 bytes, so each 100 bytes frame will store 5 measurements in total. When all the packets are sent, the UWB transceiver goes to a low-power state until the next sending state. When the program receives a 'STOP' message via UWB, it will automatically stop the accelerometer and a reset will be generated sending it back to the STANDBY mode.
- **Edge mode:** In this mode, the Sensor Node activates the accelerometer to collect data during a time window (T_{WIN}), which will vary depending on the needs of the end user. These data are processed by the Sensor Node, which performs an FFT with nFFT points to obtain a frequency domain representation of the signal we have measured in the three axes. The time window (T_{WIN}) is related to the FFT points ($nFFT$) to be obtained and the sampling frequency (f_s), where $T_{WIN} = \frac{nFFT}{f_s}$. The frequency with the highest amplitude in the spectrum resulting from the transform is sent by UWB together with the elapsed time. Once the data have been sent, the UWB transceiver will go to a low-power state.

The configuration parameters that define in which mode the Sensor Node will operate along with the UWB and accelerometer configuration parameters are received via UWB. They are sent as a 5-byte packet containing the values described below (Table 1):

Table 1. Description of parameters and settings.

Field	Description	Settings
Sampling Rate (f_s)	The ADXL355 allows easy adjustment of the sampling rate. The sampling frequencies we have used are 125, 250, 500, and 1000 Hz, which will be sufficient for the following applications	0x00 = 125 Hz 0x11 = 250 Hz 0xAA = 500 Hz 0xFF = 1000 Hz
UWB Preamble	Through this parameter, we will be able to indicate the size of the preamble of each message sent through UWB. For more robust messages, we will use longer preambles, but for high speeds, we will use short preambles.	0x00 = 64 bit 0x11 = 128 bit 0xAA = 1024 bit 0xFF = 4096 bit
UWB Data Rate	Through the data rate, we can indicate the speed of the UWB connection.	0x00 = 6800 Kbps 0xFF = 110 Kbps
Computing	Through the Computing parameter, we can indicate what type of processing we are going to work with. In Packet mode, the accelerometer samples will be sent to the Gateway in raw form periodically. In Edge mode, the data will be processed by the Sensor Node itself to send the result to the Gateway.	0x00 = Packet Mode 0xFF = Edge Mode
nFFT	Through this field, we can indicate the number of points to be used for the FFT calculation.	0x00 = 128 0x11 = 256 0xAA = 512 0xFF = 1024

With this parameterizable FW system, we have been able to perform different types of analysis for different vibration modes. As can be seen in Table 1, the ADXL355 allows the sampling rate to be easily adjusted. This value will be directly affected by the speed at which we can send the samples generated by UWB. The higher the sampling rate, the more samples will be stored in 1 s and, therefore, more packets will be sent. That is why the frequencies used in Packet mode were 125, 250, and 500 Hz, being sufficient to capture signals with frequencies up to 250 Hz. However, this problem is not seen in Edge mode since the data are stored and processed internally, without the need to send all the data to the Gateway. With both these modes, we can cover a large part of the possible tests, always taking into account the limitations of each mode.

4.2. The Gateway

- **Hardware**

Figure 6 shows the architecture of the UWB Gateway.

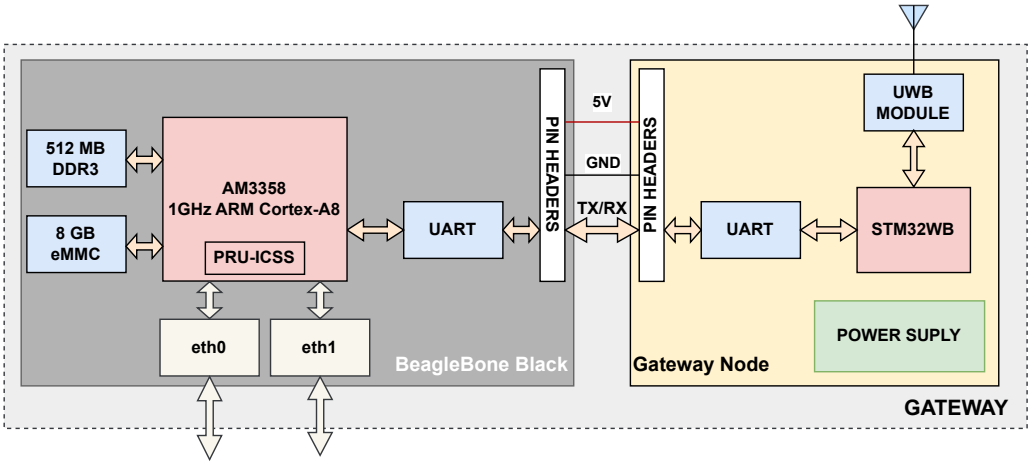

Figure 6. UWB Gateway architecture.

The Gateway consists of two components: the Gateway Node and the BeagleBone Black (BBB) [33]. The scheme is the same as the one used in [17]. The Gateway Node and the BBB are connected by GPIO pins that are used for their communication via UART.

The Gateway Node is simpler than the Sensor Node as it is mainly composed by a microcontroller (ST's STM32WB55) and a UWB integrated circuit (DW1000) [31].

Figure 7 shows a photo of the Gateway boards.

- **Firmware**

The Gateway Node application has to receive the measurements made by the Sensor Node. For this purpose, the Sensor Node, as soon as it wakes up, checks if it has received a "READY" message from the BBB via UART to start the connection with the Sensor Node via UWB. The Gateway Node receives from the BBB the configuration parameters mentioned in Table 1 to be used for both UWB and the Sensor Node's accelerometer. These parameters are sent via UWB to the Sensor Node, and then a "START" message is sent to start accelerometer measurements. The configuration parameter also indicates in which of the two existing modes the system acts with respect to the acquisition of the samples.

In the Packet mode, the Gateway node receives the measurements acquired by the Sensor Node every second through UWB. These measurements are received in packets of 100 bytes that are automatically forwarded via UART to the BBB. Once all the measurements have been reached, the Gateway Node receives a last "DONE" message and waits for the next data packet. The program runs indefinitely until the Gateway Node receives a message from the BBB through the UART connection, and consequently the 'STOP' command is sent via UWB to the Sensor Node to stop measurements. Once the program finishes, a JSON file is generated in the BBB containing the raw data of the three axes of the measurements (see Table 2).

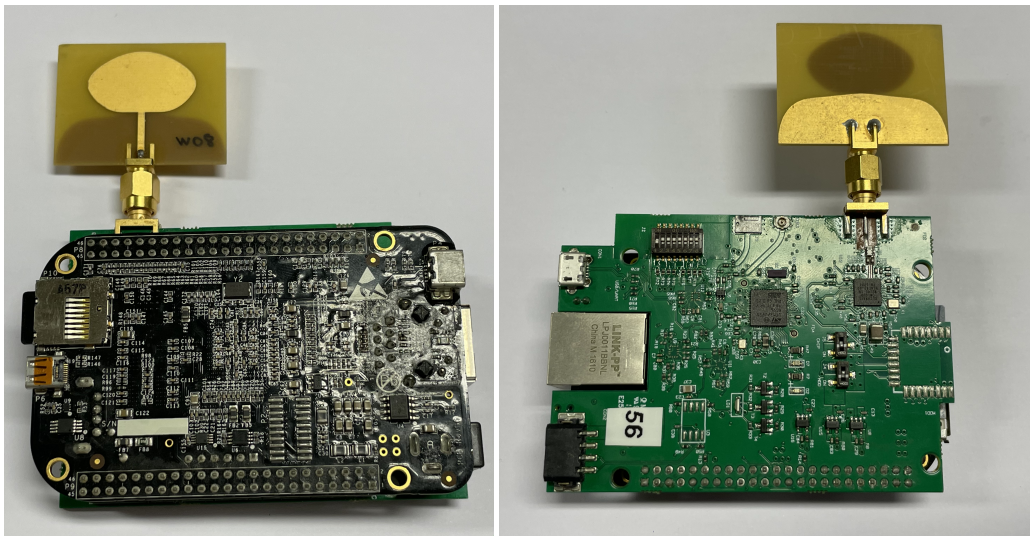

Figure 7. Gateway Node with the BBB.

Table 2. JSON file for Packet mode.

Field	Description
Name	File name
Date	Date the file was created
Samples	Total number of samples that have been collected
Sample Index	Vector containing the index of each sample at each position
X-axis	Samples obtained on the x-axis
Y-axis	Samples obtained on the y-axis
Z-axis	Samples obtained on the z-axis

In Edge mode, a single packet is received from the Sensor Node with the processing time and the peak frequency calculated through an FFT. Finally, both parameters are stored in a JSON file (see Table 3).

Table 3. JSON file for Raw mode.

Field	Description
Name	File name
Date	Date the file was created
Processing time	Time taken by the Sensor Node to process the data.
Max frequency	Peak frequency produced by the FFT implemented in the Sensor Node.

5. Power Consumption Measurements

5.1. System Setup

Figure 8 shows the configuration designed to measure the power consumption generated by the Sensor Node, based on the setup described in [17].

5.2. Methodology

As discussed in Section 4, the Sensor Node contains different modes of functionalities to perform the sending of the accelerometer data. Figure 9 shows the average power consumption profiles generated by the Sensor Node in STANDBY mode and MEASURING mode. In STANDBY mode, the process starts by activating the microcontroller, which consumes a constant power during the whole event. Afterwards, the UWB is activated to communicate with the Gateway. This fact drastically increases the power consumption. Finally, when no response is received from the Gateway, the Sensor Node goes into sleep mode, decreasing its power consumption accordingly.

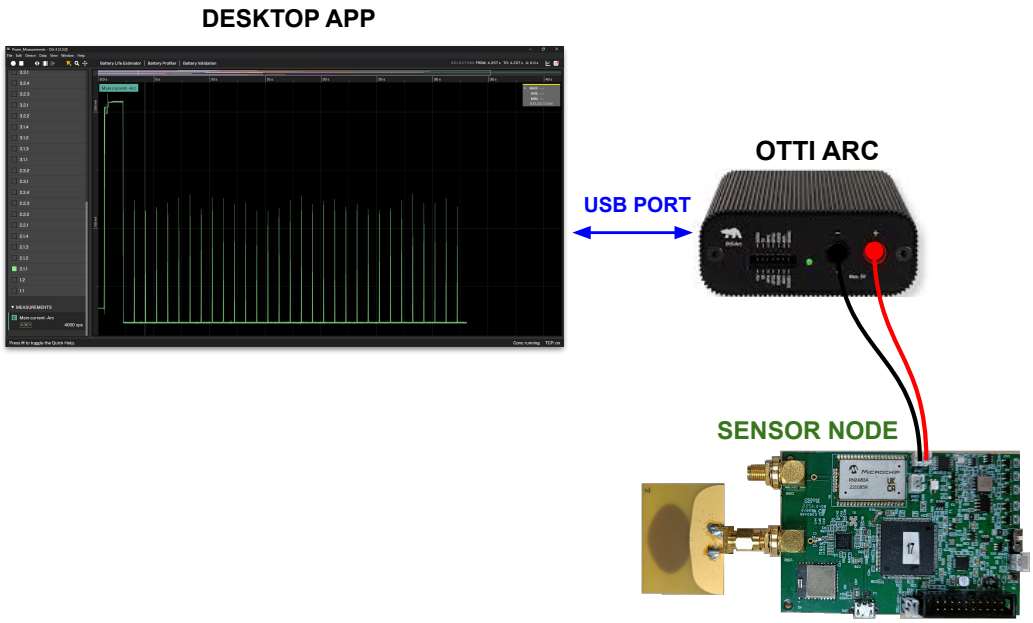

Figure 8. Setup for the power consumption measurements of the Surewave Sensor Node [17].

In Packet mode, the Sensor Node performs the same processing as in STANDBY mode, but, in this case, the Sensor Node gets a response from the Gateway and initializes the accelerometer with a further increase in the power consumption. Once the accelerometer is initialized, the Sensor Node starts an operation cycle in which the accelerometer collects data which are sent through the UWB to the Gateway. During data collection, the UWB is disabled, reducing the power consumption considerably since the UWB is the most power-demanding of the used peripherals.

On Edge mode, apart from performing the same processing as in Packet mode, the collected data are processed using the Fast Fourier Transform (FFT) implemented in the microcontroller of the Sensor Node. The power consumption of this processing will increase according to the FFT length (nFFT). The processing time and the peak frequency calculated by the FFT are sent via UWB to the Gateway.

The average power consumption in STANDBY mode is measured as a function of the cycle time T_C using Equation (1) and following the same methodology as [17]:

$$\overline{P} = \frac{(T_{ON} \times \overline{P_{ON}}) + (T_{OFF} \times \overline{P_{OFF}})}{T_C} \quad (1)$$

where, T_{OFF} and $\overline{P_{OFF}}$ represent the time and power consumed during Sleep mode, while T_{ON} and $\overline{P_{ON}}$ refer to the active process in STANDBY mode.

The average power consumed in the MEASURING mode has also been based on the cycle time T_C. In this case, T_C will be calculated from the time when the Sensor Node starts measuring concretely after the STANDBY mode.

To calculate the average power consumed on Packet mode, Equation (2) has been used.

$$\overline{P} = \frac{(T_{WIN} \times \overline{P_{WIN}}) + (T_{UWB} \times \overline{P_{UWB}})}{T_C} \quad (2)$$

where T_{WIN} and $\overline{P_{WIN}}$ are related to the time and power consumed during the accelerometer data collection, and T_{UWB} and $\overline{P_{UWB}}$ correspond to the time and power consumed during data sending by the UWB.

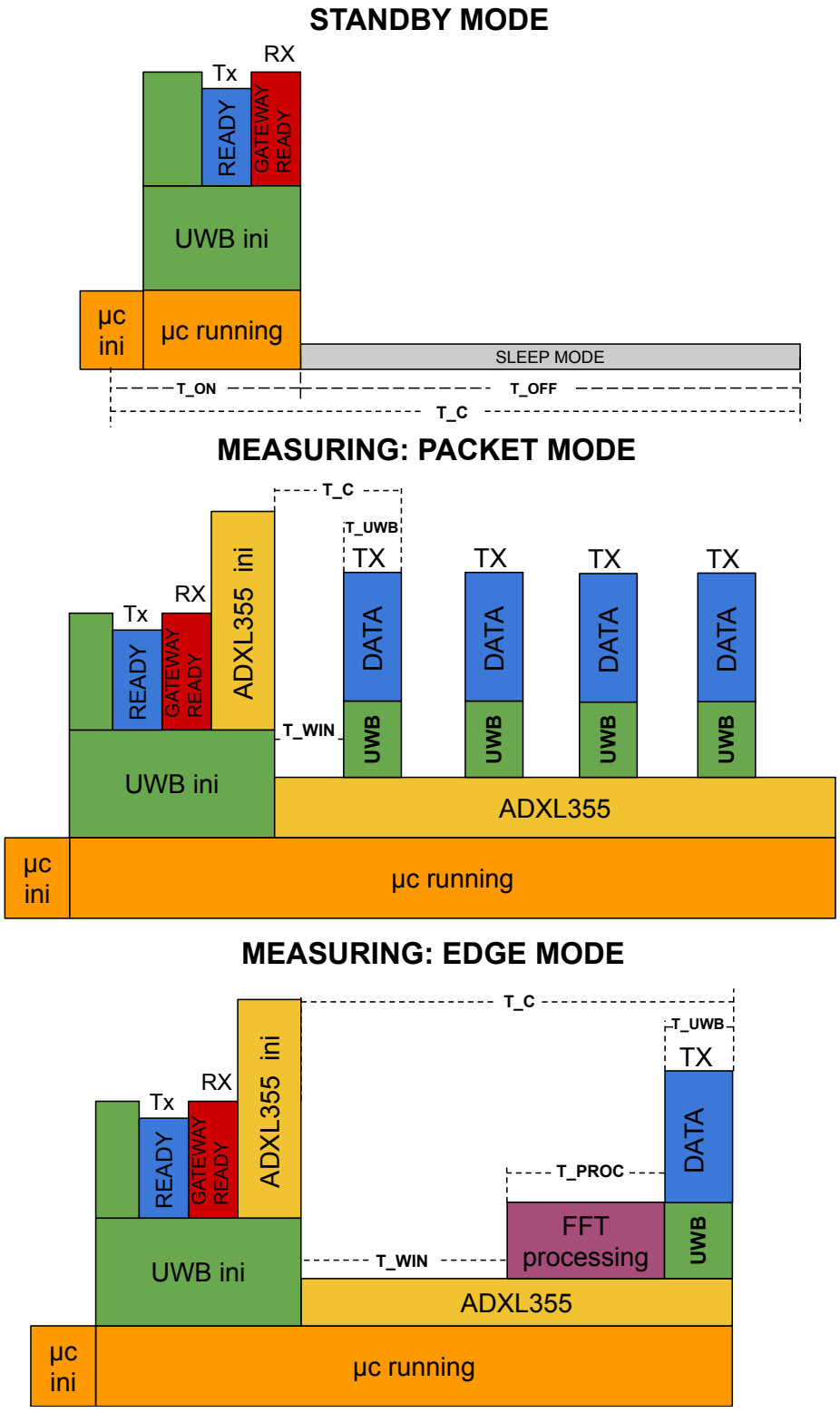

Figure 9. Power profile for Sensor Node modes.

Instead, to calculate the average power consumed in Edge mode, Equation (3) will be used. This equation uses the three stages of edge computing to calculate the average power consumed.

$$\overline{P} = \frac{(T_{WIN} \times \overline{P_{WIN}}) + (T_{PROC} \times \overline{P_{PROC}}) + (T_{UWB} \times \overline{P_{UWB}})}{T_C} \quad (3)$$

where T_{PROC} and P_{PROC} are the time and average power consumed during FFT data processing. The more data points are collected, the longer it will take to process the data; therefore, the T_{PROC} time will depend on the amount of data collected. T_{UWB} and P_{UWB} are the time and power consumed during the UWB sending process.

5.3. Sensor Node Measurements

Figure 10 illustrates the average power consumption ($\overline{P}$) of the Sensor Node when it is in STANDBY mode as a function of the duration of the off-time (T_{OFF}). It can be observed that the longer the off-time, the lower the average power consumption. As a result, the power consumption curve decreases rapidly at first and then gradually levels off as T_{OFF} increases. Equation (1) shows that ($\overline{P}$) is significantly affected by the duration of the off-time T_{OFF}, tending to become equal to P_{OFF} as T_{OFF} increases. Furthermore, the point (120, 2.40926) indicates that the average power consumption is reduced to 2.40926 mW when the STANDBY mode has 120 s of T_{OFF}.

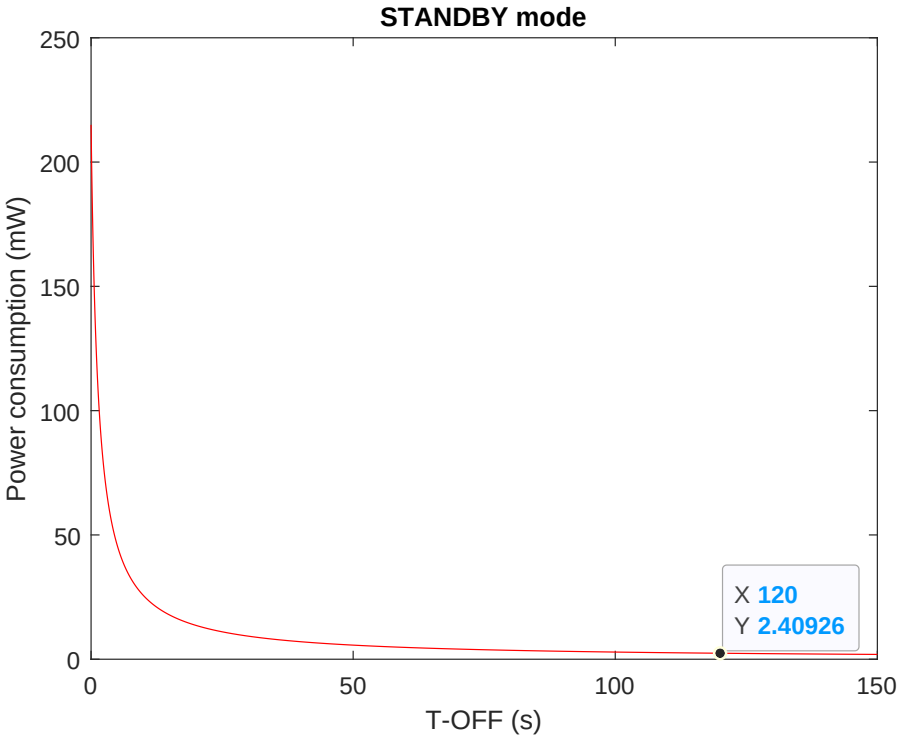

Figure 10. Average power consumption in the STANDBY mode depending on (T_{OFF}) duration.

If we consider that the Sensor Node keeps in STANDBY mode throughout the entire life of the 25.41 Wh battery and setting an off-time duration of 120 s, which is the same point as (120, 2.40926) in Figure 10, the estimated battery life is 1.204 years. However, it is crucial to note that, due to the self-discharge characteristics of batteries over time, the actual battery life will be less than the theoretical value. In the case of the battery used in SUREWAVE, an ANSMANN lithium-ion rechargeable battery, a self-discharge rate of less than 5% after one month of storage at +20 °C is indicated in [34]

Table 4 shows the average power consumption of Packet mode with different features. Measurements were performed at the frequencies of 125 Hz, 250 Hz, and 500 Hz, using preamble sizes of 64, 128, 1024, and 4096. The 500 Hz frequency is incompatible with preambles of 1024 and 4096, since it cannot perform UWB communication effectively with those preamble sizes. It is observed that the power consumption of the Sensor Node increases with the preamble length at all frequencies, with the 500 Hz frequency being the least energy-efficient. Since the Sensor Node cannot use 500 Hz at high preamble lengths, it implies that lower frequencies may be more suitable for applications requiring longer and more robust preambles, while higher frequency settings will be limited to shorter preambles

to keep communication as efficient as possible and avoid excessive power consumption. If we send the raw data as soon as a single data item is collected instead of sending by packets, the consumption would be increased six times. Therefore, that mode of operation is not interesting for low-power applications.

Table 4. Average power consumption in Packet mode with different frequencies and preamble sizes.

Preamble Size	Packet Mode 125 Hz (mW)	Packet Mode 250 Hz (mW)	Packet Mode 500 Hz (mW)
64	72.93	79.28	93.31
128	73.48	80.69	101.08
1024	142.44	216.89	-
4096	187.71	305.72	-

Figure 11 shows how the duration of the FFT data processing time (T_{PROC}) varies depending on the desired resolution in Edge mode. In this case, a comparison was made between 128, 256, 512, and 1024 FFT points. It is observed that the higher the resolution of data to be obtained, the longer it will take to process the data. However, this difference is small, with the fastest processing time being 7 ms and the slowest 12 ms. Considering that the processing time (T_{PROC}) consumes 108.9 mW per second at the Sensor Node (as shown in Table 5) and that the difference in processing time between high and low resolution is 5 milliseconds, the difference in terms of power consumption will be minimal.

Table 5. Time and power consumed in Edge states.

(a) 125 Hz with 128 FFT points		
Edge Mode	**Power (mW)**	**Duration (ms)**
uC & UWB Init	214.97	1350.9
Collecting Data	67.15	1024
Processing nFFT	108.9	7
UWB Send	266.58	1.2
(b) 250 Hz with 256 FFT points		
Edge Mode	**Power (mW)**	**Duration (ms)**
uC & UWB Init	214.97	1350.9
Collecting Data	67.15	1024
Processing nFFT	108.9	9
UWB Send	266.58	1.2

Tables 5 and 6 compare the power consumption between Edge mode and Packet mode. In Edge mode, frequencies of 125 Hz and 250 Hz with a value of 128 and 256 FFT points were used. On the other hand, in Packet mode, the same frequencies were used with a preamble of 64 and 128. The comparison was performed using these cases due to the fact that the Packet mode takes one second to cycle time (T_C). To ensure a fair comparison, the two closest cases to this T_C were chosen. It can be observed that the two modes contain the same state for collecting and sending accelerometer data. In addition, the Edge mode has to process the collected data using FFT, which will increase the power consumption for a short period of time. Moreover, the Edge mode only sends the processing time (T_{PROC}) and the maximum frequency point of the FFT, resulting in a much lower average power consumption and duration compared to the Packet mode, which sends a huge amount of raw data. Using Equations (2) and (3) to calculate the average consumption power, we obtain 151.08 mW for Edge mode and 154.55 mW for Packet mode at 125 Hz frequencies. For 250 Hz frequencies, we obtain 151.13 mW in Edge mode and 157.86 mW in Packet mode. Considering that the initialization of the UWB and the microcontroller accounts for the majority of the system's power consumption, optimizing this phase and reducing its

power usage to almost zero would make the difference between Packet and Edge modes significant. For example, if the system measures every 2 min with the same ANSMANN lithium-ion rechargeable battery at a sampling frequency of 250 Hz, the estimated battery life would be 1550.06 days in Packet mode and 1779.43 days in Edge mode, showing a difference of nearly one year between the two modes.

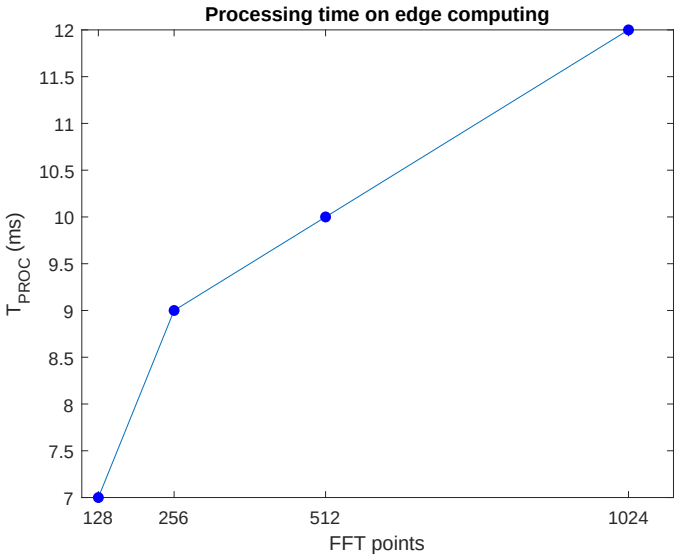

Figure 11. FFT data processing time (T_{PROC}) for different FFT points.

Table 6. Time and power consumed in Packet states.

(a) 125 Hz with a preamble of 64		
Packet Mode	**Power (mW)**	**Duration (ms)**
uC & UWB Init	214.97	1350.9
Collecting Data	67.15	971
UWB Send	266.58	29
(b) 250 Hz with a preamble of 128		
Packet Mode	**Power (mW)**	**Duration (ms)**
uC & UWB Init	214.97	1350.9
Collecting Data	67.15	932
UWB Send	266.58	68

In conclusion, it is recommended to use edge computing if the objective of the application is focused on energy efficiency. However, if the application requires manipulating the data obtained from the Sensor Node to perform different studies, it is preferable to use Packet mode where we can access the raw data for further post-processing.

6. Vibration Tests

The objective of the vibration tests is to verify the reliability of the Sensor Node. For this reason, the data obtained by the Sensor Node will be analyzed and compared with the data obtained by two wired accelerometers, such as ICP352C03 [35] and ADXL354 in two different environments.

6.1. System Setup

As explained in Section 5, the setup is formed by the Sensor Node, the Gateway Node and the BBB. The Gateway Node and the BBB (Gateway) are attached and connected to a laptop from which the application commands can be sent. The whole system was tested in two environments: at lab-scale and at a wave basin. For testing the Sensor Node near

water, a Bopla [36] waterproof housing was used to protect the Sensor Node's electronics (see Figure 12).

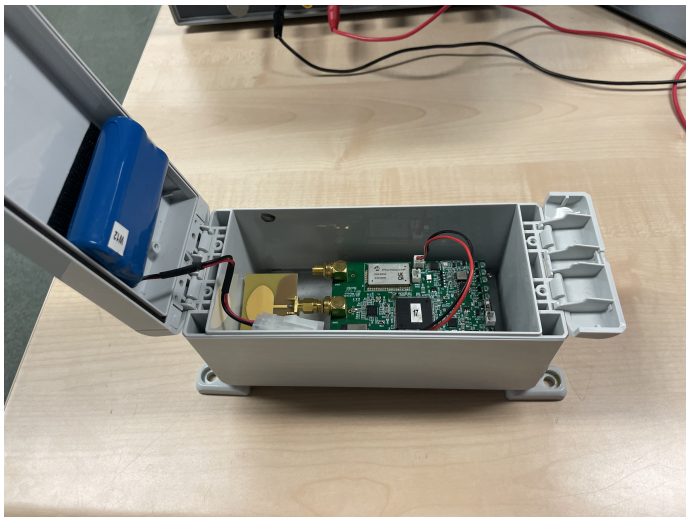

Figure 12. Sensor node fixed inside the waterproof housing with power supply battery connected.

6.2. Tests in Laboratory

To verify the reliability of the Sensor Node with a wired sensor, an initial comparison was made by creating controlled and known acceleration patterns in one dimension. These tests will make it possible to compare the data obtained by both sensors in a controlled environment.

6.2.1. Experimental Setup

A system setup was designed around the Instron machine to perform the vibration tests. The system is formed by the following blocks: the Instron machine [37], which includes a specific support designed to place our Sensor Node and the wired accelerometer; and the Gateway, as can be seen in Figure 13. Thanks to the added support, both accelerometers will be able to measure very similar accelerations at the same testing frequency. This setup will allow us to compare measurements from both accelerometers simultaneously and evaluate the accuracy of our Sensor Node.

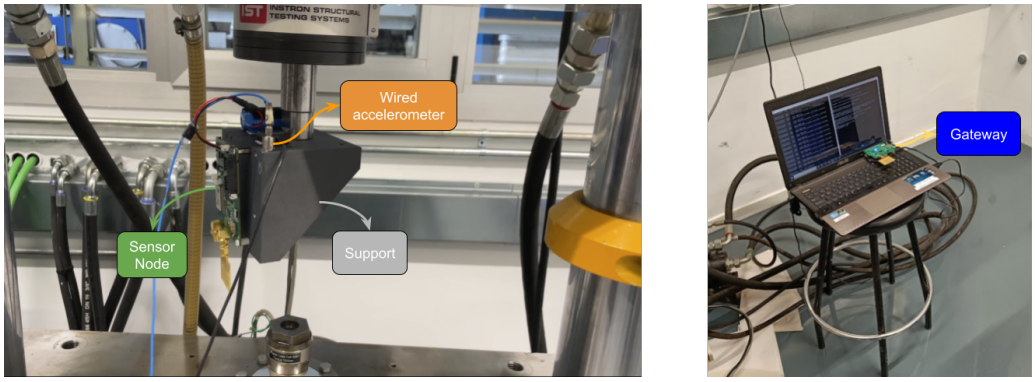

Figure 13. Implemented setup for the vibration tests.

6.2.2. Experimental Protocol

As explained in the previous sections, there are two MEASURING modes (Packet and Edge) for sending UWB data from the Sensor Node to the Gateway. In the vibration tests that were performed, the Packet mode was used to send data over the UWB to be able to analyze and compare the raw acceleration data of our Sensor Node with the wired sensor selected for each environment.

Once our Sensor Node is powered on and the Instron machine starts at the appropriate frequency, the Sensor Node is configured via the UWB to begin data collection from the accelerometer. When 100 bytes of data have been collected, they will be sent to the Gateway via UWB, and the accelerometer will continue collecting data. Meanwhile, the wired accelerometer will be collecting data at a frequency of 500 Hz for later comparison. This process was performed during one minute for each of the x-, y- and z-axes with different tests and sampling frequencies, performing a total of three different vibration tests for the three axes defined in Table 7. Also, the same tests were performed in Edge mode to verify that the frequency with the maximum amplitude corresponds with the test frequency.

Table 7. Definition of accelerometer tests.

Test Number	Test Frequency (Hz)	Sampling Frequency (Hz)	Duration (s)
1	2	125	60
2	10	250	60
3	50	500	60

6.2.3. Preprocessing and Analysis

Once the different experiments were performed, Matlab® was used to process the obtained data in the time and frequency domains. Firstly, since the Sensor Node contains 0.055% data lost due to UWB data transmission, the missing values were interpolated. This amount of lost data does not seem to affect the performance of the Sensor Node. Then, the signals from both acquisition systems are resampled to the same sampling frequency. The next step is to synchronize both signals. Then, we plot them for a time domain comparison, and find that they closely match (see Test1 example in Figure 14).

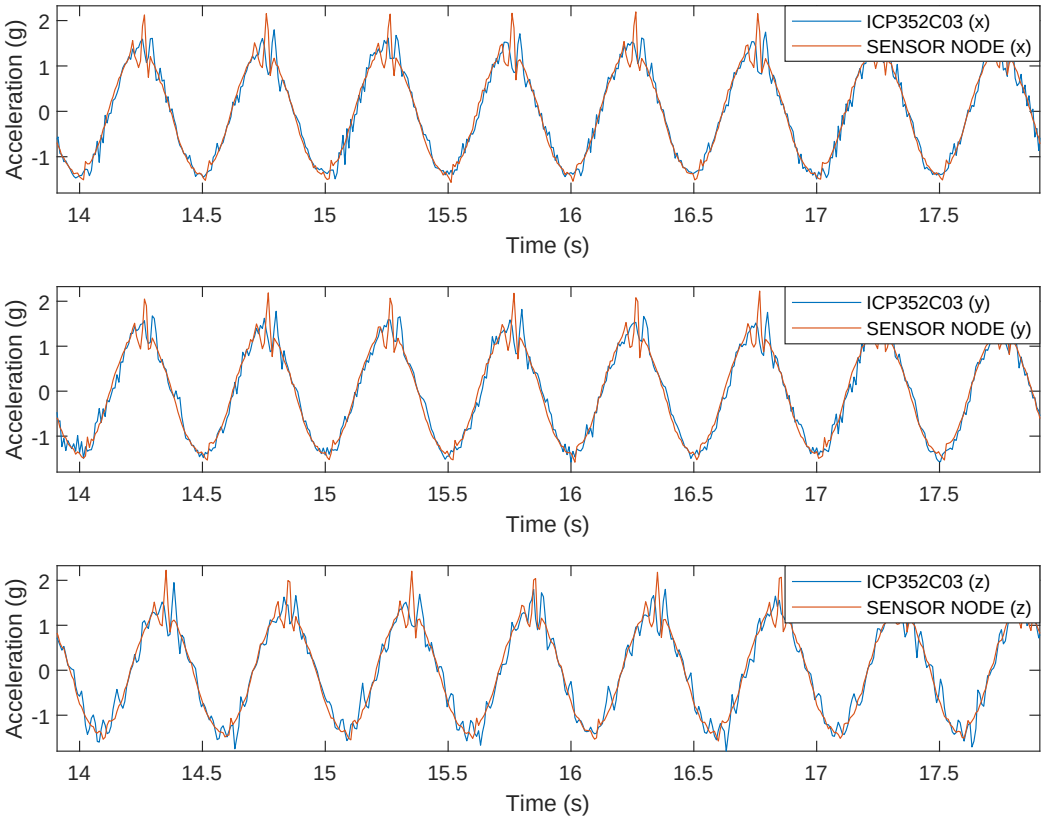

Figure 14. Comparison between Sensor Node and ICP352C03 wired sensor during vibration test with Instron machine: vibrations in X-, Y- and Z-directions.

We also perform a spectral analysis calculating and plotting the frequency spectra of both signals. They are consistent, both showing the main frequency of the lab oscillator at each trial. In Figure 15, it can be seen that the oscillating frequency is 2 Hz as Test1 was selected. The harmonics of the main frequency are also detected by both sensors. Regarding the vibration tests performed with the Edge mode, they confirm that the frequency with the maximum amplitude matches with the frequency test.

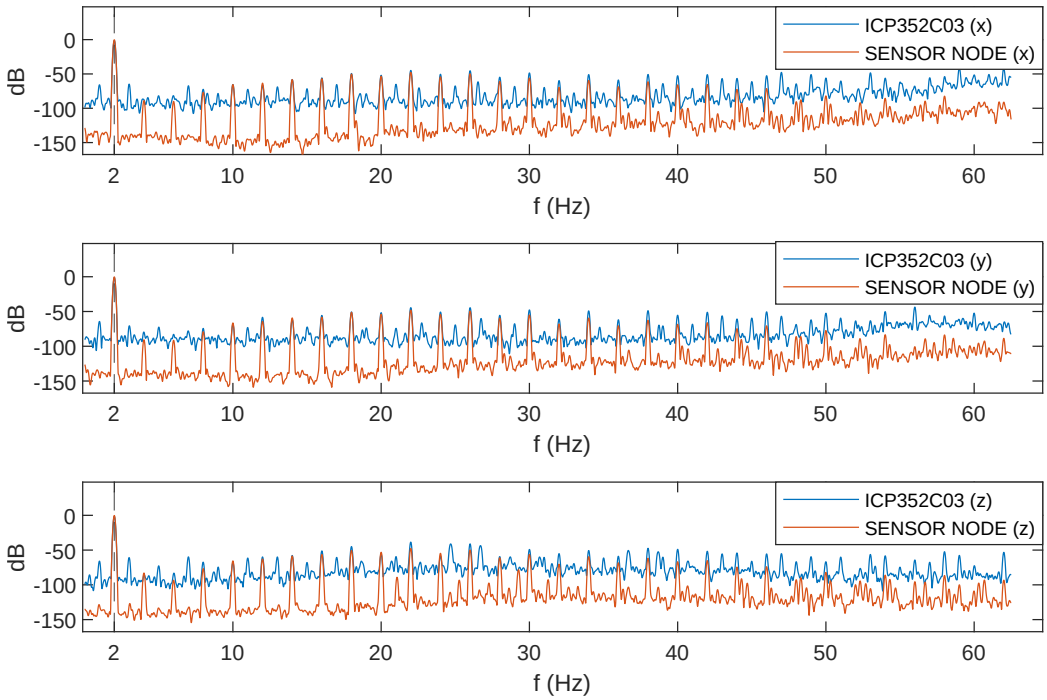

Figure 15. Spectral analysis of the ADXL355 accelerometer and the ICP352C03 accelerometer in X-, Y- and Z-directions during vibration test.

6.3. Tests at MARIN

As commented in Section 3, wave basin tests were conducted within the scope of the SUREWAVE project to analyze the hydrodynamic behavior of the FPV system in combination with a floating breakwater. These tests allowed us to make another comparison between the Sensor Node and a wired reference sensor, but this time in the setting of a realistic application. The experimental setup is presented in detail in van der Zanden et al. [30]; a summary is given in the following sections.

6.3.1. Experimental Setup

The main aim of the hydrodynamic tests was to study motions of a multi-body FPV system in mild and harsh seas, both without and with a sheltering pontoon-type floating breakwater. The tests were conducted at a geometric scale 1:10, using Froude's law of similitude to scale down the geometric, inertial, and stiffness properties of the floating bodies and FPV interconnectors from prototype designs. The dimensions and results are presented at model scale for consistency with previous sections.

The tests were performed in a rectangular wave basin with a length of 220 m, width of 4 m, and water depth of 3.6 m. The experimental setup included a floating breakwater model and a 15-body FPV model, each kept in place using soft springs (see Figure 16). Measurements included motion recordings of the floating breakwater and PV panels, mooring loads, water surface levels, and accelerations of the breakwater. In addition, all tests were logged by a camera.

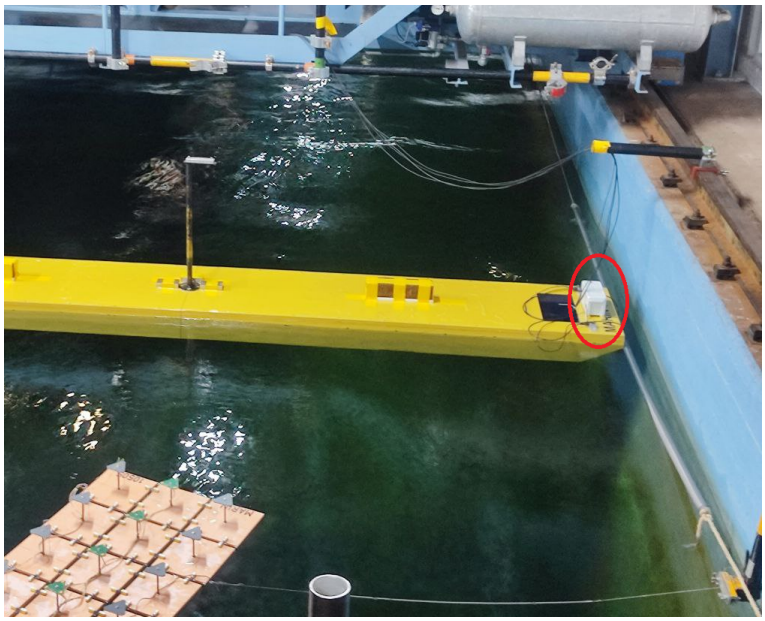

Figure 16. Sensor Node installed on the breakwater as tested during the wave basin tests.

The floating breakwater model measured 3.8 × 0.5 × 0.25 m (length × width × height), had a mass of 240 kg, and a draft of 0.20 m. The model was built of wood; the elastic properties of the concrete prototype were not considered in the model engineering. The breakwater's motions were measured using a Northern Digital Incorporated optical system at 50 Hz sampling frequency. Accelerations were measured at 200 Hz using four MARIN in-house triaxial MEMS accelerometers, each installed near a corner of the model. The motions and accelerations were acquired through the same data acquisition system which also ensured correct time synchronization. For quality control, the accelerations at the model's centre of gravity derived from the four accelerometers were compared to accelerations obtained through double differentiation of the optical motion measurements, showing an excellent match.

In addition to MARIN's instrumentation, CEIT deployed the Sensor Node proposed in this paper (see the highlighted device on the right side in Figure 16). Because the MARIN and CEIT accelerometers are not collocated, the triaxial acceleration at the location of CEIT's sensor was instead computed based on the recordings and known positions of the four MARIN wired accelerometers. This allows a direct comparison between both types of sensors.

6.3.2. Experimental Program

The floating breakwater was tested in three different long-crested irregular wave conditions, as summarized in Table 8. The first condition is a so-called white noise wave, with constant spectral energy between periods of 0.76 to 3.73 s (0.27 to 1.32 Hz). The other two conditions are JONSWAP wave conditions that are representative for real storm conditions at sea. The two conditions differ in terms of significant wave height and peak period. The highest wave condition (JONSWAP 2) corresponds to a 1 y return period storm condition at a field site in the Baltic Sea. Both JONSWAP conditions resulted in wave overwash and slamming loads due to wave breaking onto the breakwater model.

The natural modes of motion of the floating breakwater were quantified through motion decay tests, in which the motion response following an initial offset was measured. The main hydrodynamic modes of interest are the vertical motions (heave) and the rotations along the longitudinal axis (roll) of the model. The heave and roll natural frequencies were 0.81 and 0.76 Hz, respectively.

Finally, hammer tests in still water were performed to quantify the structural response (vibration mode) of the model near the location of the CEIT sensor.

Table 8. Test program of MARIN floating breakwater wave basin tests

Test ID	Description	Significant Wave Height [m]	Peak Period [s]
34018_11_003_001_01	White noise	0.067	0.76–3.73
34018_11_004_001_01	JONSWAP 1	0.101	1.30
34018_11_005_001_01	JONSWAP 2	0.306	2.35

6.3.3. Preprocessing and Analysis

Firstly, identically to the experiment in the previous section, the values lost in transmission are accounted for through interpolation, for which, in this case, only 0.03% of the data were lost. Then, the CEIT's signals are resampled to have the same sampling rate as the Marin's signals. The next step is to synchronize the signals, since the recording trigger for each instrumentation was independent. For this purpose, the cross-correlation (R_{xy}) of the signals is calculated until a reasonable maximum lag value m is achieved. The lag value m, where the R_{xy} is maximum, corresponds to the time difference between the onset of recording between both acquisition systems, and thus the signals are time-shifted. At this point, plotting allows us to visually inspect them, from which we found they closely match (see Figure 17).

Apart from the time-domain analysis, a spectral analysis was performed. The frequency spectrum of both signals was calculated and compared. Since the signals closely match in the time domain, we expect their spectra to do the same. This is, in fact, what can be seen in Figure 18.

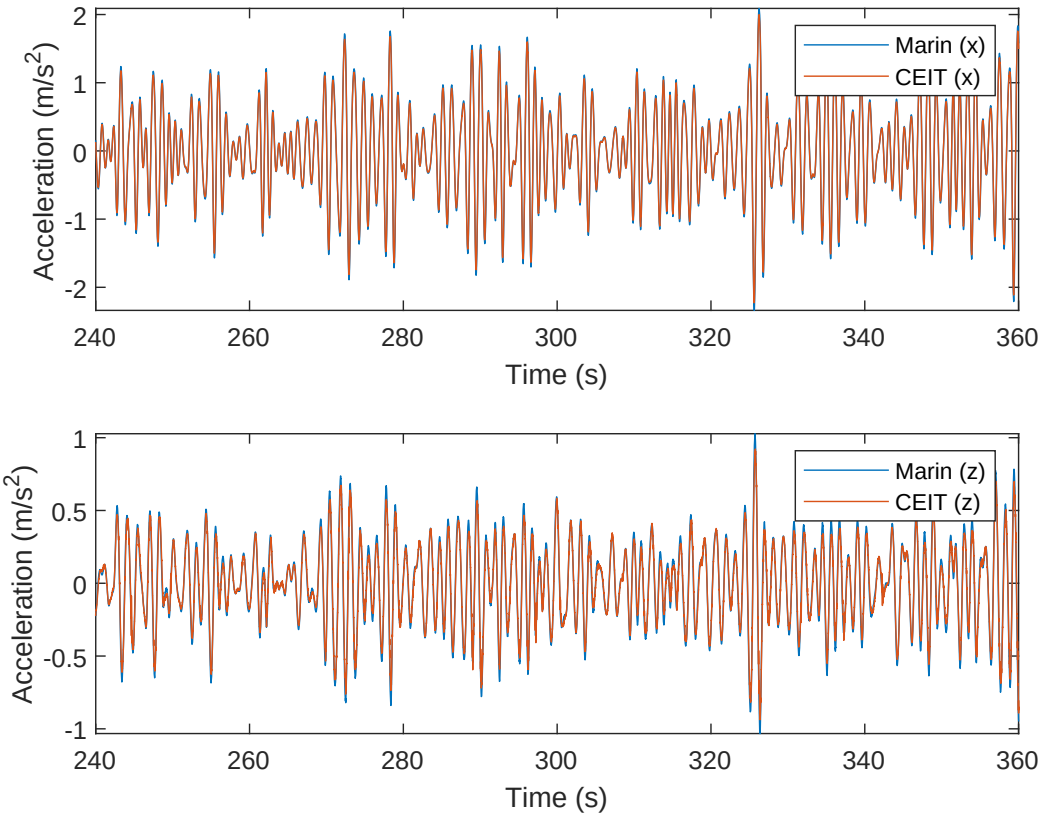

Figure 17. Comparison between CEIT's sensor and MARIN's sensor during experiment 34018_11_003_001_01: vibrations in X- and Z-directions.

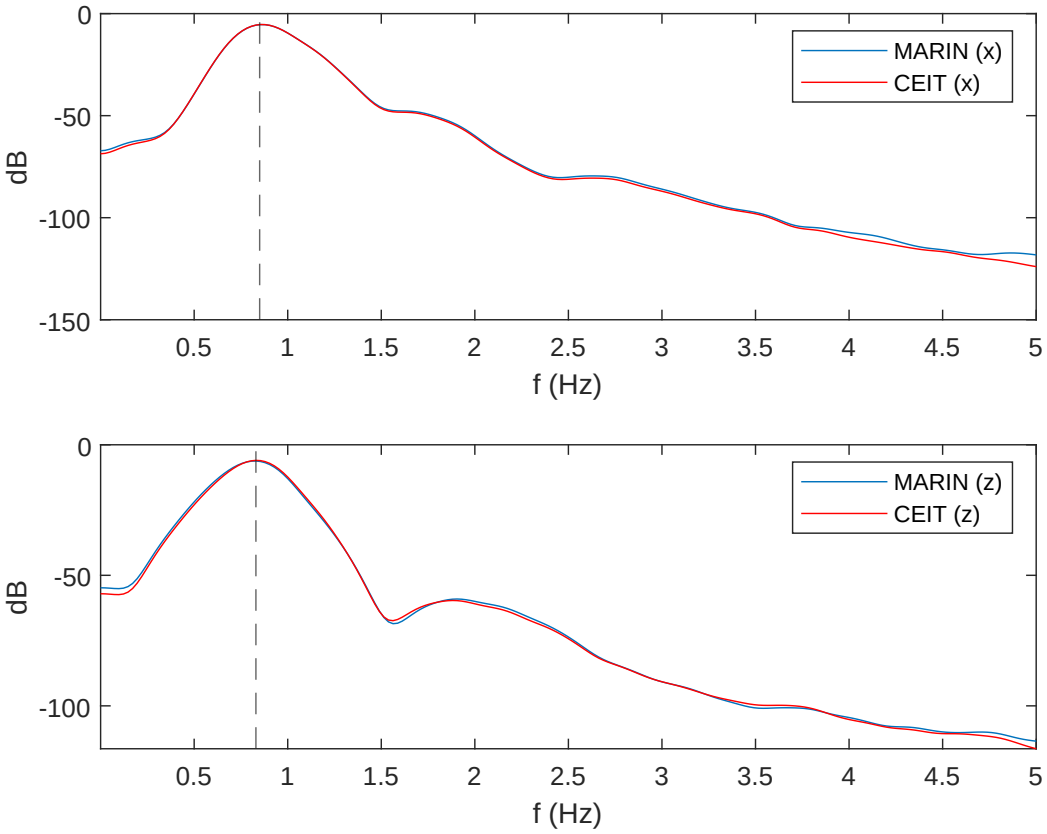

Figure 18. Comparison between the spectral analysis of CEIT's sensor and MARIN's sensor in X- and Z-directions in the 34018_11_003_001_01 experiment.

7. Conclusions

The growth of renewable offshore energy, especially in wind power, requires cost reduction and improved efficiency in offshore wind farms. The use of remote condition monitoring systems allows for structural health assessment, prevention of failures, effective maintenance scheduling, and optimization of equipment lifespan, despite environmental and logistical challenges.

The literature review highlights the preference for Wireless Sensor Networks (WSNs) in offshore platform monitoring systems due to their scalability and ease of expansion. Impulse Radio Ultra-Wideband (IR-UWB) technology is emphasized for its flexibility and robustness in challenging environments. It also identified WSNs based on accelerometers, analyzing their performance in capturing dynamic data. Optimization and real-world suitability are highlighted as key areas for improvement in these systems.

A wireless Sensor Node offers simplified installation and enhanced flexibility due to the absence of cables. It can lead to long-term savings by reducing labor and material expenses associated with cables. Durability is improved as cable wear and damage is eliminated, requiring less maintenance, and it is easier to scale up or expand to monitor multiple points simultaneously. On the other hand, the large data from vibration sensors need energy-intensive wireless transmission, making wireless accelerometers dependant on batteries. Energy-saving strategies and smart data management techniques are utilized to improve the efficiency of Sensor Nodes. The proposed Sensor Node behavior can be remotely configured to either transmit raw data for further analysis or process data at the edge, enhancing energy efficiency. By choosing between the two modes, we can address a wide range of potential applications, while always considering the limitations inherent to each mode. On the one hand, in the case of Packet mode, lower sampling frequencies may be more suitable for applications requiring longer and more robust UWB preambles. Conversely, higher sampling frequency settings will be limited to shorter UWB preambles to maintain communication as efficiently as possible and avoid excessive power

consumption. However, this issue does not occur in Edge mode since the data are stored and processed internally, without the need to send all the data to the Gateway. On the other hand, if the application requires analyzing data from the Sensor Node for various studies, it is preferable to use Packet mode, which allows access to raw data for further post-processing. In contrast, edge computing is recommended if the application's goal is energy efficiency, where the system can yield a battery life of up to more than 4 years by performing a measurement every 2 min.

Controlled acceleration patterns were used to compare data from a wired sensor and the proposed Sensor Node, ensuring reliability through controlled testing in a laboratory environment. Spectral analysis of both signals revealed consistency, both showing the main frequency of the lab oscillator at each trial. Also, vibration tests in Edge mode confirmed the matching frequency with the maximum amplitude observed.

Finally, under the SUREWAVE project and with the collaboration of the MARIN Institute, wave basin tests were conducted to assess the hydrodynamic behavior of a multi-body Floating Photo-Voltaic (FPV) system. This system includes an external floating breakwater structure designed to protect the FPV structure from severe wave loads. These tests offered a valuable opportunity to assess the performance of the proposed method for offshore platforms and compare its performance with the wired acquisition system used by MARIN for hydrodynamic analysis. To simulate the typical motion of a breakwater, the tests were conducted at frequencies below 5 Hz. Both time-domain and spectral analyses were performed, demonstrating a close match with the data provided by the wired sensor. This confirms the efficacy of the proposed Sensor Node in this kind of application.

In summary, many works in the literature are either proof of concepts that are not optimized in terms of power consumption and data handling, or they are not suited for challenging and remote environments. In response, this paper presents a specialized wireless Sensor Node utilizing an accelerometer, specifically designed for remote vibration monitoring. It features efficient data transmission, resilience to harsh marine conditions, low energy consumption, and edge-processing capabilities. Additionally, it has been tested in a relevant environment, making it ready for deployment.

8. Future Work

To enhance the profitability of offshore wind energy as a leading renewable option, it is essential to implement advanced intelligent monitoring systems like the one proposed. Although the proposed Sensor Node has a long battery life, the goal is to reduce maintenance costs by eliminating the need to replace sensor batteries. Therefore, future work will focus on equipping the Sensor Node with an energy-harvesting system to prolong battery life. To achieve this, a study should be conducted to determine the type of harvester that can capture the most energy. Additionally, implementing AI, machine learning processes, or smart policies to manage the Sensor Node's operation mode could be beneficial. The ultimate objective is to make this Sensor Node self-sustainable.

In this work, the capability of the Sensor Node to process data at the edge is evaluated. In line with this research, we are developing new measurement concepts, methods, and algorithms to determine structural health. Since the proposed Sensor Node has proven capable of performing complex operations while maintaining low power consumption, future work will include measuring additional structural parameters, beyond just accelerations, and fusing them using these new complex algorithms to assess structural health.

Finally, future work will include deploying the proposed system on an offshore structure for an extended period. A large measurement campaign will be carried out to both extract meaningful information related to the structure and observe the trend of the battery.

Author Contributions: Conceptualization, A.C. (Ainhoa Cortés); formal analysis, A.C. (Ainhoa Cortés), M.L. and A.I.; funding acquisition, A.C. (Ainhoa Cortés); investigation, A.C. (Ainhoa Cortés), M.L., A.C. (Adrián Carrasco) and I.F.; methodology, A.C. (Ainhoa Cortés), M.L., A.C. (Adrián Carrasco), I.F. and J.V.d.Z.; project administration, A.C. (Ainhoa Cortés); software, M.L., I.F. and A.C. (Adrián Carrasco); supervision, A.C. (Ainhoa Cortés) and A.I.; validation, M.L., I.F., A.O. and J.V.d.Z.; writing—original draft, A.C. (Ainhoa Cortés), M.L., I.F. and A.O.; writing—review and editing, A.C. (Adrián Carrasco), A.I., A.O., M.L., A.C. (Ainhoa Cortés) and J.V.d.Z. All authors have read and agreed to the published version of the manuscript.

Funding: The present study is part of the SUREWAVE project, funded by the European Union with GA No. 101083342. The views and opinions expressed are however those of the author(s) only and do not necessarily reflect those of the European Union or European Climate, Infrastructure and Environment Executive Agency (CINEA). Neither the European Union nor the granting authority can be held responsible for them.

Data Availability Statement: The raw data supporting the conclusions of this article will be made available by the authors on request.

Acknowledgments: This work was made possible through the collaboration between CEIT and all the SUREWAVE partners, with special thanks to MARIN in this instance.

Conflicts of Interest: Author Joep Van der Zanden was employed by the company Marin. The remaining authors declare that the research was conducted in the absence of any commercial or financial relationships that could be construed as a potential conflict of interest.

Abbreviations

The following abbreviations are used in this manuscript:

BBB	BeagleBone Black
DDR3	Double Data Rate version 3
eMMC	eMbedded Multimedia Card
FFT	Fast Fourier Transform
FPV	Floating Photo-Voltaic
FW	FirmWare
GPIO	General Purpose Input-Output
IC	Integrated Circuit
IEEE	Institute of Electrical and Electronics Engineers
IoT	Internet of Things
IR-UWB	Impulse Radio Ultra-Wideband
JSON	JavaScript Object Notation
JONSWAP	Joint North Sea Wave Project
LCoE	Levelized Cost of Energy
LDO	Low-DropOut
MEMS	MicroElectroMechanical systems
OWF	Offshore Wind Farms
PHY	Physical Layer
PRU	Programmable Real-Time Unit
PV	PhotoVoltaics
RAM	Random Access Memory
RGB	Red Green Blue
RoI	Return on Investment
SHM	Structural Health Monitoring
SMA	SubMiniature version A
SPI	Serial Peripheral Interface
SRAM	Static Random Access Memory

SWD	Serial Wire Debug
TI	Texas Instruments
UART	Universal Asynchronous Receiver-Transmitter
USB	Universal Serial Bus
UWB	Ultra-Wideband
WSN	Wireless Sensor Network

References

1. Leung, D.Y.; Yang, Y. Wind energy development and its environmental impact: A review. *Renew. Sustain. Energy Rev.* **2012**, *16*, 1031–1039. [CrossRef]
2. Snyder, B.; Kaiser, M.J. Ecological and economic cost-benefit analysis of offshore wind energy. *Renew. Energy* **2009**, *34*, 1567–1578. [CrossRef]
3. EUR-Lex—52021DC0550—ES—EUR-Lex. Available online: https://eur-lex.europa.eu/legal-content/EN/TXT/?uri=CELEX:52021DC0550 (accessed on 26 March 2024).
4. Mazur, D.C.; Kay, J.A.; Mazur, K.D. Advancements in Vibration Monitoring for the Mining Industry. *IEEE Trans. Ind. Appl.* **2015**, *51*, 4321–4328. [CrossRef]
5. Zhao, L.; Zhou, Y.; Matsuo, I.; Korkua, S.K.; Lee, W.J. The Design of a Holistic IoT-Based Monitoring System for a Wind Turbine. In Proceedings of the IEEE/IAS 55th Industrial and Commercial Power Systems Technical Conference (I&CPS), Calgary, AB, Canada, 5–8 May 2019. [CrossRef]
6. Nguyen, N.T.; Sbartaï, Z.M.; Lataste, J.F.; Breysse, D.; Bos, F. Assessing the spatial variability of concrete structures using NDT techniques—Laboratory tests and case study. *Constr. Build. Mater.* **2013**, *49*, 240–250. [CrossRef]
7. Vaghefi, K.; Oats, R.C.; Harris, D.K.; Ahlborn, T.T.M.; Brooks, C.N.; Endsley, K.A.; Roussi, C.; Shuchman, R.; Burns, J.W.; Dobson, R. Evaluation of Commercially Available Remote Sensors for Highway Bridge Condition Assessment. *J. Bridge Eng.* **2012**, *17*, 886–895. [CrossRef]
8. Kilic, G.; Unluturk, M.S. Testing of wind turbine towers using wireless sensor network and accelerometer. *Renew. Energy* **2015**, *75*, 318–325. [CrossRef]
9. Popeanga, C.; Dobrescu, R.; Cristov, N. Smart monitoring and controlling of wind turbines farms based on wireless sensors networks. In Proceedings of the 1st International Conference on Systems and Computer Science (ICSCS), Lille, France, 29–31 August 2012. [CrossRef]
10. Ciang, C.C.; Lee, J.R.; Bang, H.J. Structural health monitoring for a wind turbine system: A review of damage detection methods. *Meas. Sci. Technol.* **2008**, *19*, 122001. [CrossRef]
11. Qiao, W.; Lu, D. A Survey on Wind Turbine Condition Monitoring and Fault Diagnosis—Part I: Components and Subsystems. *IEEE Trans. Ind. Electron.* **2015**, *62*, 6536–6545. [CrossRef]
12. reza Akhondi, M.; Talevski, A.; Carlsen, S.; Petersen, S. Applications of Wireless Sensor Networks in the Oil, Gas and Resources Industries. In Proceedings of the 24th IEEE International Conference on Advanced Information Networking and Applications, Perth, Australia, 20–23 April 2010; pp. 941–948. [CrossRef]
13. Zhixin, F.; Yue, Y. Condition health monitoring of offshore wind turbine based on wireless sensor network. In Proceedings of the 10th International Power & Energy Conference (IPEC), Ho Chi Minh City, Vietnam, 12–14 December 2012; pp. 649–654. [CrossRef]
14. Martinez-Luengo, M.; Kolios, A.; Wang, L. Structural health monitoring of offshore wind turbines: A review through the Statistical Pattern Recognition Paradigm. *Renew. Sustain. Energy Rev.* **2016**, *64*, 91–105. [CrossRef]
15. Wehs, T.; Janssen, M.; Koch, C.; von Cölln, G. System architecture for data communication and localization under harsh environmental conditions in maritime automation. In Proceedings of the IEEE 10th International Conference on Industrial Informatics, Beijing, China, 25–27 July 2012; pp. 1252–1257. [CrossRef]
16. Wang, P.; Yan, Y.; Bouzid, O.; Ding, Z. Investigation of Wireless Sensor Networks for Structural Health Monitoring. *J. Sens.* **2012**, *2012*, 156329. [CrossRef]
17. Guisasola, A.; Cortés, A.; Cejudo, J.; da Silva, A.; Losada, M.; Bustamante, P. Reliable and Low-Power Communications System Based on IR-UWB for Offshore Wind Turbines. *Electronics* **2022**, *11*, 570. [CrossRef]
18. Azim, A.; Matin, M.; Asaduzzaman; Amin, N. UWB Technology for WSN Applications. In *Novel Applications of the UWB Technologies*; IntechOpen Limited: London, UK, 2011. [CrossRef]
19. Zhu, L.; Fu, Y.; Chow, R.; Spencer, B.; Park, J.; Mechitov, K. Development of a High-Sensitivity Wireless Accelerometer for Structural Health Monitoring. *Sensors* **2018**, *18*, 262. [CrossRef] [PubMed]
20. Komarizadehasl, S.; Lozano, F.; Lozano-Galant, J.A.; Ramos, G.; Turmo, J. Low-Cost Wireless Structural Health Monitoring of Bridges. *Sensors* **2022**, *22*, 5725. [CrossRef]
21. Veluthedath Shajihan, S.A.; Chow, R.; Mechitov, K.; Fu, Y.; Hoang, T.; Spencer, B. Development of Synchronized High-Sensitivity Wireless Accelerometer for Structural Health Monitoring. *Sensors* **2020**, *20*, 4169. [CrossRef]
22. Wondra, B.; Malek, S.; Botz, M.; Glaser, S.; Grosse, C. Wireless High-Resolution Acceleration Measurements for Structural Health Monitoring of Wind Turbine Towers. *Data-Enabled Discov. Appl.* **2019**, *3*, 4. [CrossRef]

23. Ahuir Torres, J.; Bausch, N.; Farrar, A.; Webb, S.; Simandjuntak, S.; Nash, A.; Thomas, B.; Muna, J.; Jonsson, C.; Mathew, D. Benchmarking parameters for remote electrochemical corrosion detection and monitoring of offshore wind turbine structures. *Wind Energy* **2019**, *22*, 857–876. [CrossRef]
24. Losada, M.; Cortés, A.; Irizar, A.; Cejudo, J.; Pérez, A. A Flexible Fog Computing Design for Low-Power Consumption and Low Latency Applications. *Electronics* **2021**, *10*, 57. [CrossRef]
25. Agarwal, D.; Kishor, N. An approach to real-time fault detection in health monitoring of offshore wind-farms. In Proceedings of the IEEE Asia Pacific Conference on Wireless and Mobile, Bali, Indonesia, 28–30 August 2014; pp. 247–253. [CrossRef]
26. Losada, M.; Adin, I.; Perez, A.; Ramírez, R.C.; Mendizabal, J. Connected Heterogenous Multi-Processing Architecture for Digitalization of Freight Railway Transport Applications. *Electronics* **2022**, *11*, 943. [CrossRef]
27. Väänänen, O.; Hämäläinen, T. Requirements for Energy Efficient Edge Computing: A Survey. In Proceedings of the 18th International Conference (NEW2AN 2018) and the 11th Conference (ruSMART 2018), St. Petersburg, Russia, 29 September 2018; pp. 3–15. [CrossRef]
28. Jiang, C.; Fan, T.; Gao, H.; Shi, W.; Liu, L.; Cérin, C.; Wan, J. Energy aware edge computing: A survey. *Comput. Commun.* **2020**, *151*, 3–15. [CrossRef]
29. Morabito, R. Virtualization on Internet of Things Edge Devices with Container Technologies: A Performance Evaluation. *IEEE Access* **2017**, *5*, 8835–8850. [CrossRef]
30. van der Zanden, J.; Bunnik, T.; Cortés, A.; Delhaye, V.; Kegelart, G.; Pehlke, T.; Panjwani, B. Wave Basin Tests of a Multi-Body Floating PV System Sheltered by a Floating Breakwater. *Energies* **2024**, *17*, 2059. [CrossRef]
31. DW1000 User Manual from Decawave. Available online: https://www.decawave.com/dw1000/usermanual/ (accessed on 17 June 2024).
32. Analog Devices Inc. ADXL354/ADXL355 3-Axis MEMS Accelerometers. Available online: https://www.mouser.es/new/analog-devices/adi-adxl354-adxl355-accelerometers/ (accessed on 17 June 2024).
33. BeagleBone® Black. Available online: https://www.beagleboard.org/boards/beaglebone-black (accessed on 17 June 2024).
34. ANSMANN 2447-3033-20. Available online: https://es.farnell.com/en-ES/ansmann/2447-3033-20/battery-li-ion-7ah-3-63v/dp/2777013/ (accessed on 17 June 2024).
35. ACCELEROMETER, ICP® Model 352C03 Product Specifications. Available online: https://www.pcb.com/contentStore/docs/pcb_corporate/vibration/products/specsheets/352c03_e.pdf (accessed on 9 July 2024).
36. Bocube | Caja, policarbonato UL 94 V0, Unicolor. Available online: https://www.bopla.de/es/division-de-envolventes/bocube/pc-ul-94-v0-unicolor/caja-policarbonato-ul-94-v0-unicolor/b-180809-pc-v0-7035 (accessed on 18 June 2024).
37. Elastomeric-Testing System MHF. Available online: https://www.instron.com/pt-br/-/media/literature-library/applications/2006/01/elastomeric-testing-system-mhf.pdf (accessed on 7 August 2024).